CYCLONE GLOBAL NAVIGATION SATELLITE SYSTEM (CYGNSS)

Algorithm Theoretical Basis Document Level 3 Ocean Microplastic Concentration	

UM Doc. No.	**148-0402**
SwRI Doc. No.	**N/A**
Revision	**Rev 2**
Date	**17 June 2024**
Contract	**NNL13AQ00C**

Algorithm Theoretical Basis Documents (ATBDs) provide the physical and mathematical descriptions of the algorithms used in the generation of science data products. The ATBDs include a description of variance and uncertainty estimates and considerations of calibration and validation, exception control and diagnostics. Internal and external data flows are also described.

SPACE PHYSICS RESEARCH LABORATORY

NASA

CYCLONE GLOBAL NAVIGATION SATELLITE SYSTEM (CYGNSS)

Algorithm Theoretical Basis Document Level 3 Ocean Microplastic Concentration		
	UM Doc. No.	**148-0402**
	SwRI Doc. No.	**N/A**
	Revision	**Rev 2**
	Date	**17 June 2024**
	Contract	**NNL13AQ00C**

Prepared by: Madeline Evans, University of Michigan Date: 6/17/2024
Chris Ruf, University of Michigan
Gopal Sundaram, University of Michigan

Approved by: _____ Date: 17 June 2024
Chris Ruf, CYGNSS Principal Investigator

Approved by: _____ Date: 17 June 2024
Darren McKague, CYGNSS Cal/Val Science Lead

Released by: _____ Date: 17 June 2024
Darren McKague, CYGNSS Cal/Val Science Lead

SPACE PHYSICS RESEARCH LABORATORY

REVISION NOTICE

Document Revision History		
Revision	**Date**	**Changes**
PRE-RELEASE DRAFT	29 Sept 2021	n/a
INITIAL RELEASE	29 Sept 2021	
REVISION 1	10 April 2024	The general approach is the same as the initial release. Updates to the empirical parametric model parameters were made so the algorithm is compatible with the v3.2 Level 1 data product that is used as input to the algorithm. Specific changes include: - Changes in Figures 3-6 & 9 due to updated CYGNSS data from v 2.1 to v 3.2. - Updated from GDAS winds to ERA5 winds. - Control Regions were changed, along with the methodology of which model fit is used. - MSS Anomaly to Microplastic Concentration fits updated
REVISION 2	17 June 2024	Minor changes

Table of Contents

1 Introduction and Background

1.1 Ocean Microplastics Science Background

Plastic debris accounts for an estimated 80-85% of litter in marine environments [1]. These plastics will rarely biodegrade. Instead, larger plastics will continuously break down into smaller pieces, eventually becoming microplastics [1-5]. Primarily, microplastics are measured using samples captured by plankton or neuston nets towed on the ocean surface, a method known as net trawling [5, 6]. This method is crucial for the collection of ground truth data. However, on a global scale, spatial coverage is limited, and temporal fluctuations are not adequately resolved. Remote sensing is an important step towards the large-scale monitoring of marine microplastics [7].

1.2 Science Background and Objectives

This data product reports ocean microplastic number density (#/km^2) derived from the observed suppression of wind-driven ocean surface roughness. On annual timescales over large areas, the roughness suppression is highly correlated with global models of microplastic concentration [8]. The wave damping mechanism which produces the roughness suppression is believed to be caused primarily by surfactant films acting as tracers for the surface-level microplastics [9, 10].

2 Algorithm Description

2.1 Algorithm Overview

A schematic for the CYGNSS microplastic retrieval algorithm is shown in Figure 1. First, CYGNSS mean square slope (MSS) measurements of ocean surface roughness are matched up to independent measurements of wind speed. MSS anomalies are deviations from the expected ocean surface roughness, derived from ambient wind speeds using an empirical model for the wind-MSS relationship in low microplastic regions. MSS anomalies are used to resolve microplastic concentration using a log-linear model derived from the relationship between annual MSS anomaly averages and modelled microplastic concentrations. Resultant microplastic concentration retrievals are binned into 30-day, 1^{o}x1^o spatiotemporal cells and the geometric average, geometric standard deviation, and sample size of retrievals are computed. Bins are incremented by 1 day and 0.25^o to produce this monthly data product.

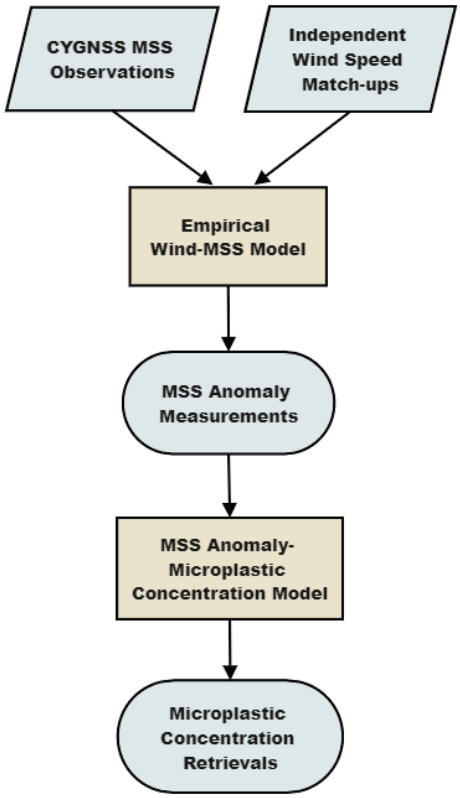

Figure 1. Data flow schematic of the CYGNSS ocean microplastic retrieval algorithm

2.2 Input Data Description

1. MSS input data are from CYGNSS Level 2, Version 3.2 [11]. These MSS measurements are time-tagged with 25 km resolution. Input data used for the initial release of the L3 microplastic concentration data product covers 8 August 2018 – 29 March 2024. Input data have been filtered using the Fully Developed Seas quality control flags.
2. Wind speed data is sourced from the ECMWF Reanalysis v5 (ERA5) Neutral Wind Speed Dataset. ERA5 10-meter reference winds have 1-hour, 0.2° resolution [12]. Ocean vector wind components (u, v) are used to derive wind speed as $\sqrt{u^2 + v^2}$. Winds are matched up using a linear interpolation in time of the ERA5 winds that are closest in location to CYGNSS.

2.3 Microplastic Model Data Description

The relationship between MSS anomaly and microplastic concentration is derived using microplastic concentration data produced by the van Sebille model described in [5]. However, each of the three models (van Sebille, Lebreton, and Maximenko) were used for validation analysis. These models use differing source, sink, particle transport functions, and run times to model the global distribution of buoyant small plastic debris concentrations with 1°x1° resolution.

Details of the three models can be found in Table 1. Despite the model differences, resulting ocean microplastic concentrations are similar, as demonstrated in Figure 2.

Table 1. Descriptions of the source functions, transport algorithms, sink functions, and run times of global microplastic models [5]

Model	Van Sebille	Lebreton	Maximenko
Source Function	Coastlines with concentrations that are proportional to human population within 200 km of the coast. Concentration is scaled by each country's mismanaged waste.	Major river mouths, along coastlines, and on major shipping routes. Higher concentrations are proportional to human population and urban development. Concentration increases over time with global plastic production.	Initial uniform distribution over global ocean.
Transport Algorithm	Debris are transported using particle travel probabilities calculated from a historical global set of satellite tracked drifter buoys from the NOAA Global Drifter Program.	Debris are transported using ocean velocity fields from the HYCOM global circulation model.	Debris are transported using particle travel probabilities calculated from a historical global set of satellite tracked drifter buoys from the NOAA Global Drifter Program.
Sink Function	N/A	N/A	Particles "wash ashore" when entering coastal grid cells.
Model Run Time	50 years	30 years	10 years

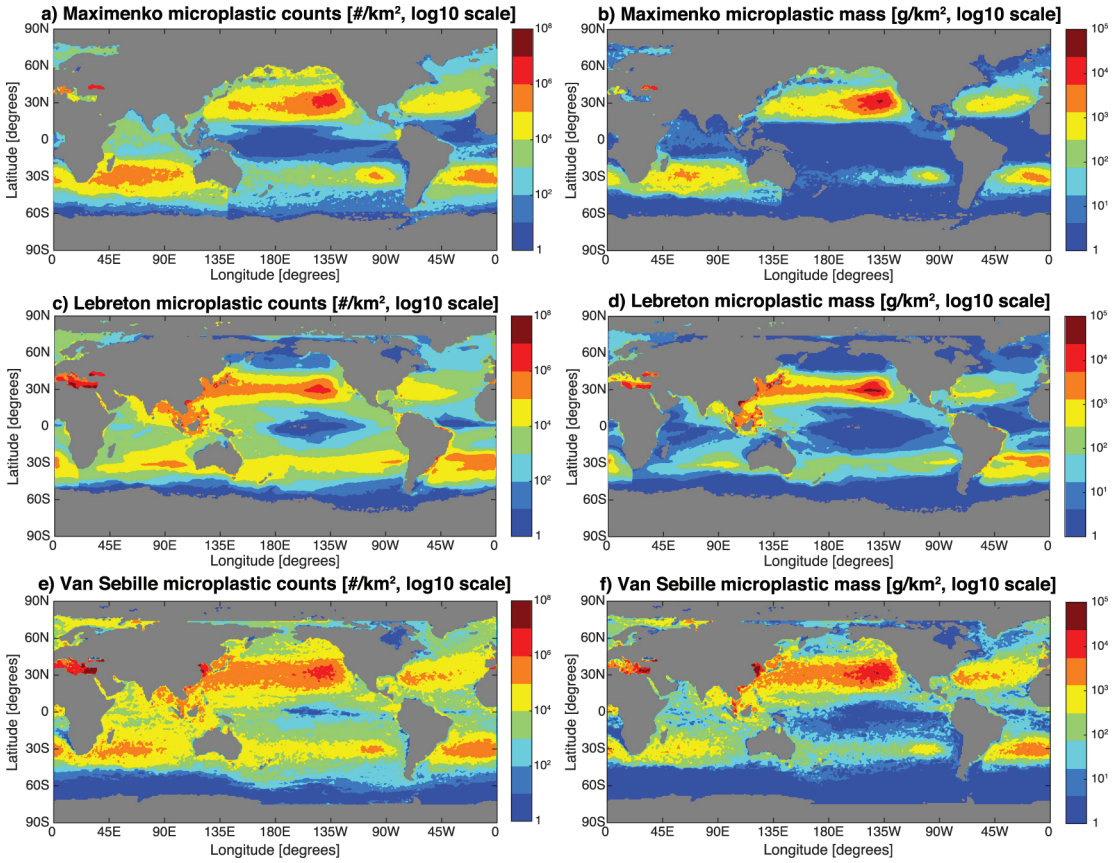

Figure 2. Global distributions of microplastic mass (g/km^2) and number density (#/km^2) from the van Sebille, Lebreton, and Maximenko models [5]. Model results of microplastic number density are used to train and validate the CYGNSS ocean microplastic retrieval algorithm.

2.4 Plastic Retrieval Algorithm Description

2.4.1 Empirical Wind-MSS Model

2.4.1.1 Modelled MSS and MSS Anomaly

Modelled MSS is calculated using an empirical model that generates MSS from the ambient wind speed, given by

$$MSS_{mod} = -0.000225U^2 + 0.006465U - 0.005962 \qquad (1)$$

where U is the ocean surface wind speed referenced to 10 m height in a neutral stability atmosphere, as reported by ERA5. Equation (1) is based on the best fit polynomial to the data in Figure 3. Parameters are fit to one year of CYGNSS MSS observations and matched-up ERA5 wind speed measurements within a control region. A density scatter plot of the match-up

samples, together with the best-fit empirical model derived from them, are displayed in Figure 3.

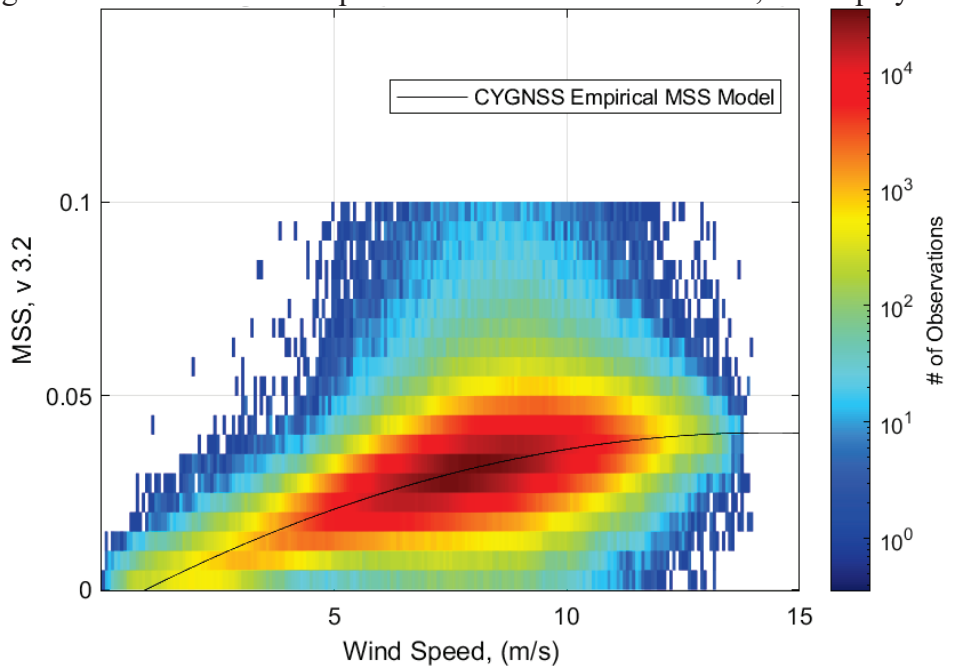

Figure 3. One year of MSS observations and collocated ERA5 wind speed from within the control region of historically low microplastic concentration are shown in a density scatter plot. The cutoff at 0.1 in the MSS is from the CYGNSS Level 2 processing algorithm. These data are used to train the empirical model (Equation 1), highlighted by the solid black line. Deviations of MSS observations from this relationship constitute the MSS anomalies used to detect microplastic concentration in other regions.

The control region is used to establish a baseline relationship in clean-water areas where low concentrations of microplastic debris are expected [5]. This control region is composed of two sub-regions CR1 [8-17° S, 100°-120° W] and CR2 [5°-10° S, 7°-33° W], shown in Figure 4. Note the intertropical convergence zone (ITCZ) is necessarily excluded from the control regions due to anomalous atmospheric stability conditions there.

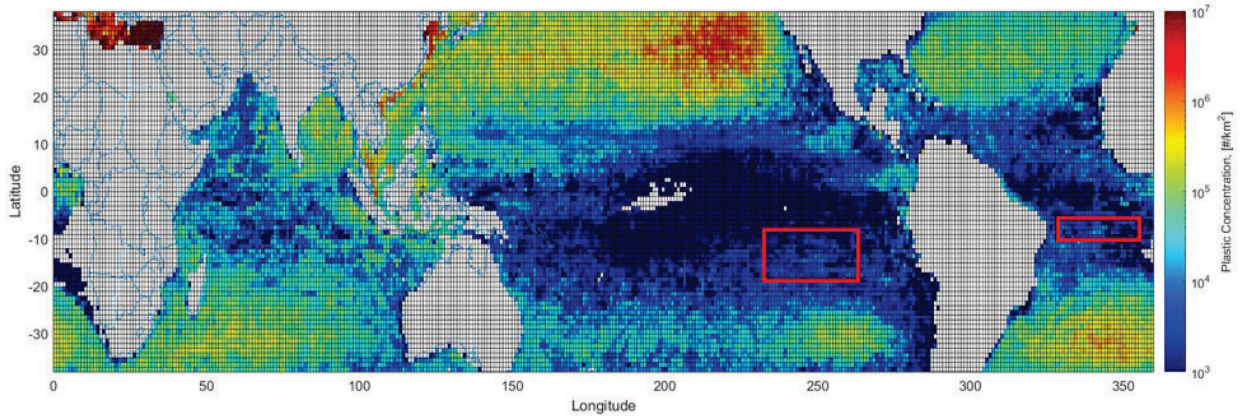

Figure 4. Global microplastic number density in #/km^2 from the van Sebille model [5]. Control regions contain low microplastic concentrations and are denoted by red boxes. Observations from within these regions used to train the empirical MSS-wind relationship.

The MSS anomaly at any location, either within or outside of the control regions, is defined as:

$$MSS_{anom} = \frac{MSS_{obs} - MSS_{mod}}{MSS_{mod}} \qquad (2)$$

2.4.1.2 Wind Speed Range

Microplastic concentration observations are derived from MSS anomalies provided the wind speed lies within the range 5-11 m/s. Within this range, there is a consistent correlation between MSS anomaly and microplastic concentration. Figure 5 shows correlation coefficients between MSS anomaly and microplastic concentration binned by collocated wind speed. The wind speed data was taken from the control regions defined in Figure 4 and the North Pacific Garbage Patch [30°-38°N, 125°-175°W]. Defining this wind range does not significantly reduce the samples size, as this range is representative of a large majority of samples. 5-11 m/s is used due to it being the common operational range for all three models.

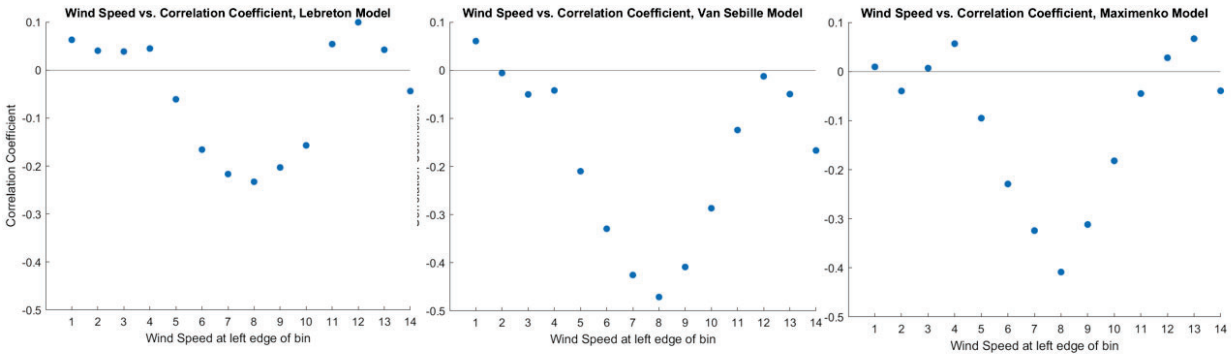

Figure 5. Correlation coefficients are binned and averaged according to collocated wind speeds to determine the operational range, 5-11 m/s, for ocean microplastic detection. Wind speed data from the Control Regions and the North Pacific Gyre was used to make a clear determination of the operational range.

2.4.2 MSS Anomaly-Microplastic Concentration Model

Microplastic concentration is inferred from MSS anomaly using the MSS Anomaly-Microplastic Concentration Model given by

$$\rho = 4320\exp(-12.06 MSS_{anom}) \quad (3)$$

where ρ is the microplastics number density in units of #/km^2. This relationship is derived from a map of one-year averages of MSS anomalies spatially matched up to global microplastic concentration models. The MSS anomaly map and each microplastic model has 1°x1° resolution. The latitude range of the matchup is 37°N-37°S.

Equation (3) uses a log-linear regression of the van Sebille model data and annual roughness suppression data. Figure 6 displays the relationship between van Sebille microplastic concentration and CYGNSS MSS anomaly averages. The blue line denotes the geometric average of microplastic concentration binned by MSS anomaly matchups (0.005 width). The central range of the data lies between MSS anomaly values of -0.045 and 0.0243 (shown by two vertical lines). Here, the sample size in each MSS anomaly bin is N ≥ 600, corresponding to a 95% confidence level and a 4% margin of error.

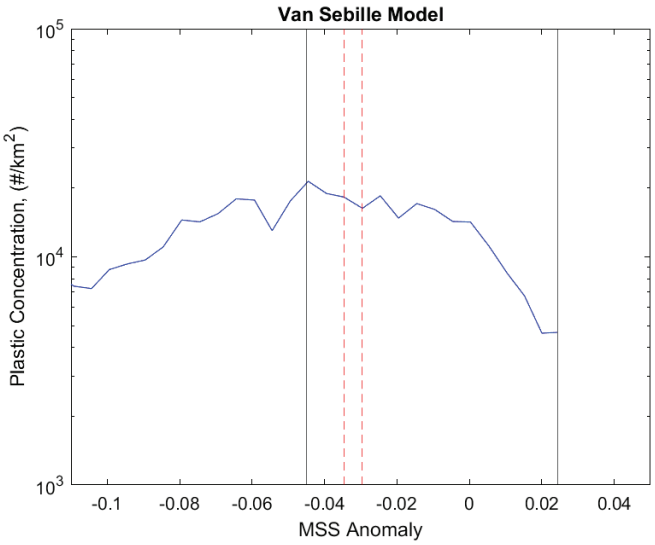

Figure 6. A comparison between MSS anomaly and van Sebille model predictions of microplastic number density (#/km^2). The solid blue line shows geometrically averaged microplastic counts within MSS anomaly bins. Data within the central range, contained inside the vertical black lines, is used to train the retrieval algorithm. The area enclosed by the red dashed lines is the MSS Anomaly bin with the highest number of samples, demonstrating that most data is accounted for in this range.

2.4.3 Microplastic Detection Algorithm Validation

2.4.3.1 Comparison to Training Model

Equation 3 is applied to the annual average map of MSS anomalies to produce a map of retrieved microplastic concentrations. Note that due to the log-linear nature of Equation 3, equivalent retrievals are made by arithmetically averaging MSS anomalies, then applying Equation 3 to the map, and by first applying Equation 3 to individual MSS anomalies then geometrically averaging microplastic concentrations within the same spatiotemporal bin. Figure 7 shows a) the map of annual average MSS anomaly, b) microplastic concentrations from the van Sebille model, and c) the resultant annual retrieval map of microplastic concentrations. Areas of high and low concentrations are indicated respectively by the red and white boxes.

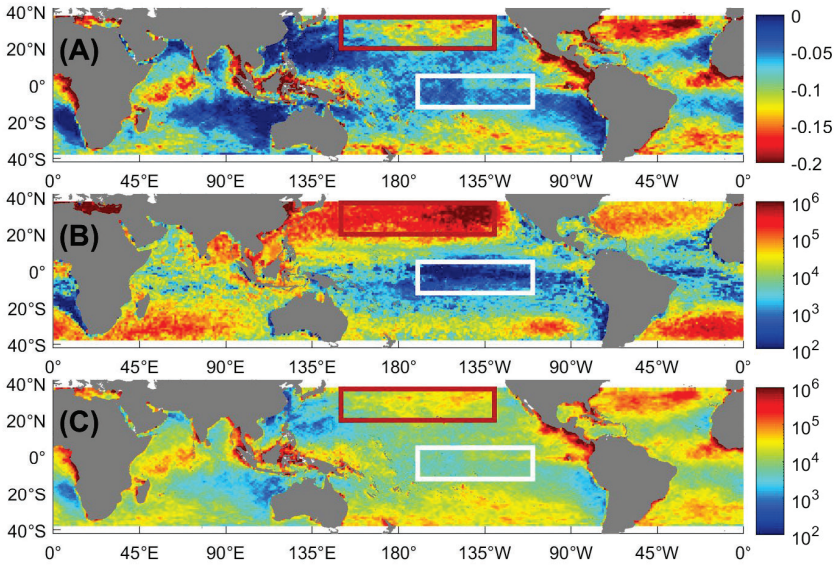

Figure 7. Global maps of (A) annual average MSS anomaly observations, (B) microplastic number density (#/km^2) from the van Sebille model, and (C) annual average microplastic number density (#/km^2) retrieved using CYGNSS. High and low microplastic concentration regions are indicated by the red and white boxes, respectively.

Figure 8a shows the density scatter plot of matched-up model and retrieval concentrations. The highest density of matchups is found near the 1:1 line of perfect agreement. However, significant deviations are also present in this comparison and may be caused by retrieval errors, variables that are not accounted for in the current algorithm, or errors in the model itself. Note also that the model has significantly lower concentration values. This may in part be attributed to retrieval limitations from ITCZ atmospheric conditions in equatorial latitudes, where low microplastic concentrations are primarily found. Figure 8b shows a histogram of the difference between log10(#/km2) concentrations from the model and retrieval. The black line denotes the mean difference, or bias,

between model and retrieval, equal to 0.002. The RMS difference between the model and retrieval is 1.003 log10(#/km2).

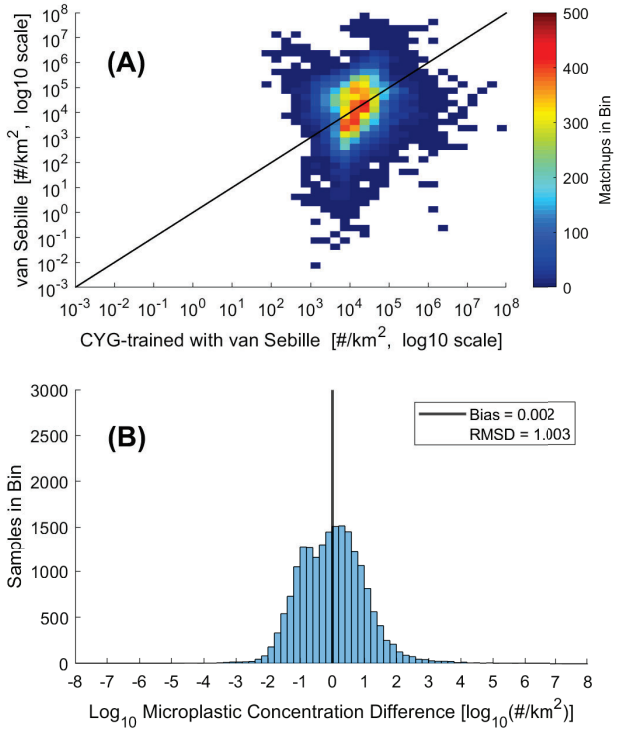

Figure 8. (A) Density scatter plot of spatially matched microplastic concentration (#/km^2) from the van Sebille model and annual average of CYGNSS retrievals trained with the van Sebille model. The highest density of samples surrounds the 1:1 line of perfect agreement. (B) Histogram of the difference in microplastic concentration matchups with respect to log$_{10}$(#/km^2) values. The bias (mean difference) is 0.002 and the RMS difference is 1.003.

2.4.3.2 Dependence on Training Model

The same log-linear regression method was used to train annual microplastic retrievals using all three models. The relationship between matchups of the annual MSS anomaly map and microplastic concentrations from all three models are shown in Figure 9. Within the central range of each plot, the microplastic concentrations monotonically increase as MSS anomaly decreases, indicative of increased wave damping. The Pearson correlation coefficients of each log-linear regression in the central range are 0.95 (van Sebille), 0.94 (Lebreton) and 0.92 (Maximenko).

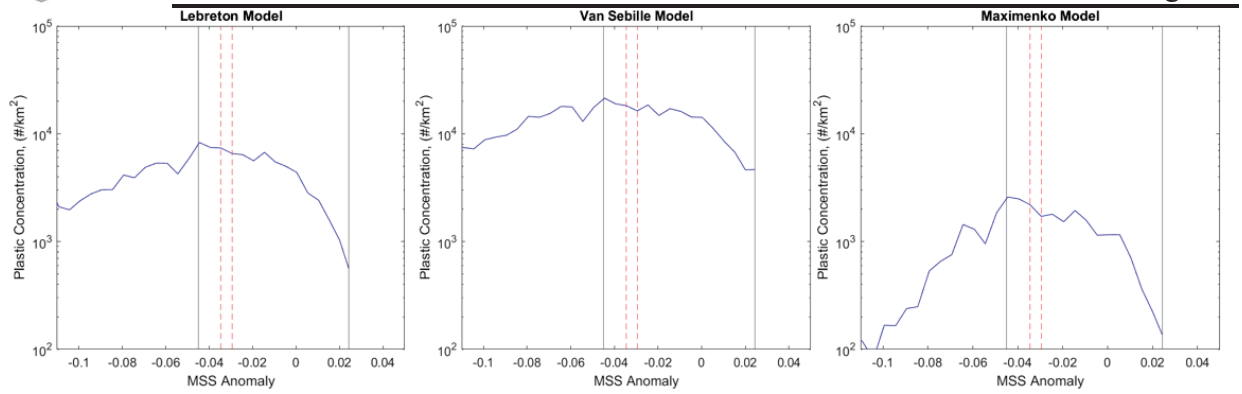

Figure 9. Comparisons similar to Figure 6 between MSS anomaly and predictions of microplastic number density (#/km^2) from the (A) Lebreton, (B) van Sebille, and (C) Maximenko models. The vertical black lines indicate the edges of the central range of data used to train the retrieval algorithms. The area enclosed by the red dashed lines indicates the MSS Anomaly bin with the highest number of samples, helping demonstrate that most data is accounted for in this range.

To validate use of the van Sebille model in training the final algorithm, the annual microplastic concentration retrieval maps trained with the van Sebille and Lebreton models are compared to the models themselves. The Maximenko model and the retrieval trained with it were excluded because the Maximenko model predictions are significantly lower than the other two model predictions. This is likely due to the sink mechanism present only in the Maximenko model, which allows plastics to exit the system at coastlines.

Validity is evaluated by comparing the difference statistics from retrievals and models to inter-model difference statistics as an independent evaluation of inherent uncertainties. Table 2 contains these difference statistics. The mean and RMS differences are calculated with respect to the log10(#/km^2) microplastic concentration in all cases due to the logarithmic distribution of concentration data. The retrievals have very low mean difference when compared to the models with which they are trained (i.e. the retrieval trained with van Sebille vs. the van Sebille model), which is to be expected. When comparing retrievals to the model with which they are not trained (i.e., the retrieval trained with van Sebille vs. the Lebreton model) the mean difference stays relatively low, using the inter-model mean difference as a standard. The inter-model RMSD is slightly lower than that of the retrievals compared to either model, suggesting that the difference can be primarily attributed to uncertainties in the models themselves, with a small additional uncertainty resulting from errors in the retrieval algorithm.

Table 2. Statistics comparing the differences between retrievals and reference models.

Product Under Test	Reference Model			
	van Sebille		Lebreton	
	Mean Diff*	RMS Diff*	Mean Diff*	RMS Diff*
van Sebille Model	--	--	0.471	0.906
Lebreton Model	-0.471	0.906	--	--
Retrieval trained with van S.	0.002	1.003	0.474	1.307
Retrieval trained with Leb.	-0.494	1.147	-0.023	1.244

*All statistics are with respect to the $\log_{10}$ (#/km^2) of the microplastic number density

2.5 Output Data Product Description

Ocean microplastic concentrations are produced by geometrically averaging individual microplastic concentration retrievals within 30-day, 1x1° resolution bins. A timestamp coordinate is at the center of each 30-day bin and is incremented by 1 day. Latitude and longitude coordinates lie in the center of each 1°x1° spatial bin and are incremented by 0.25°. The latitude and longitude ranges of this L3 product are 37°N-37°S and 0E-359.75°E, respectively.

Geometric averaging is used due to the logarithmic distribution of microplastic concentration observations. These averages are calculated according to

$$GM[\rho] = \exp\left(\frac{\sum_{i=1}^{N} \ln(\rho_i)}{N}\right) \qquad (4)$$

where GM[ρ] is the geometric mean of microplastic number density observations (ρ_1, ρ_2, ... ρ_N) in units of #/km^2.

This product also contains sample size, N, and geometric standard deviation of microplastic concentration within each spatiotemporal bin. Geometric standard deviation is found using

$$GSD[\rho] = \exp\left(\sqrt{\frac{\sum_{i=1}^{N} (\ln(\rho_i) - \bar{\rho})^2}{N}}\right) \qquad (5)$$

where GSD[ρ] is the geometric standard deviation of microplastic number density observations (ρ_1, ρ_2, ... ρ_N). It is important to note that GSD[ρ] is a unitless factor that is either multiplied with or divides the GM[ρ] to describe the distribution of data. Data within one standard deviation of the mean exist within the range of $GM[\rho]\ ^{\times}/_{\div}\ GSD[\rho]$.

3 References

[1] H. S. Auta, C. U. Emenike, S. H. Fauziah, "Distribution and importance of microplastics in the marine environment: A review of the sources, fate, effects, and potential solutions" Environment International 102, 165-176 (2017). doi: 10.1016/j.envint.2017.02.013

[2] D. K. A. Barnes, R. Galgani, R. C. Thompson, M. Barlaz, "Accumulation and fragmentation of plastic debris in global environments" Phil. Trans. R. Soc. B. 364, 1985-1998 (2009). doi: 10.1098/rstb.2008.0205

[3] C. G. Alimba, C. Faggio, "Microplastics in the marine environment: Current trends in environmental pollution and mechanisms of toxicological profile" Environmental toxicology and Pharmacology 68, 61-74 (2019). doi: 10.1016/j.etap.2019.03.001

[4] A. Cózar, F. Echevarría, J. Ignacio González-Gordillo, X. Irigoien, B. Úbeda, S. Hernández-León, Á. T. Palma, S. Navarro, J. García-de-Lomas, A. Ruiz, M. L. Fernández-de-Puelles, C. M. Duarte, "Plastic debris in the open ocean" PNAS 111, 10239-10244 (2014). doi: 10.1073/pnas.1314705111

[5] E. van Sebille, C. Wilcox, L. Lebreton, N. Maximenko, B. D. Hardesty, J. A. van Franeker, M. Eriksen, D. Siegel, F. Galgani, K. L. Law, "A global inventory of small floating plastic debris" Environ. Res. Lett. 10, 124006 (2015). doi: 10.1088/1748-9326/10/12/124006

[6] K. M. Viršek, A. Palatinus, Š.Koren, M. Peterlin, P. Horvat, A. Kržan, "Protocol for microplastics sampling on the sea surface and sample analysis" J. Vis. Exp. 118, e55161 (2016). doi: 10.3791/55161

[7] N. Maximenko, P. Corradi, K. L. Law, E. van Sebille, S. P. Garaba, R. S. Lampitt, et al., "Toward the integrated marine debris observing system" Front. Mar. Sci. 6, 2296-7745 (2019). doi: 10.3389/fmars.2019.00447

[8] M. C. Evans and C. S. Ruf, "Toward the Detection and Imaging of Ocean Microplastics with a Spaceborne Radar" IEEE Transactions on Geoscience and Remote Sensing, 1-6 (2021). doi: 10.1109/TGRS.2021.3081691

[9] E. van Sebille, S. Aliani, K. L. Law, N. Maximenko, J. M. Alsina, A. Bagaev, et al, "The physical oceanography of the transport of floating marine debris" Environ. Res. Lett. 15, 023003 (2020). doi: 10.1088/1748-9326/ab6d7d

[10] D'Asaro, Eric A, Shcherbina, Andrey Y, Klymak, Jody M, Molemaker, Jeroen, Novelli, Guillaume, Guigand, Cedric M, Haza, Angelique C, et al. "Ocean convergence and the dispersion of flotsam" Proceedings of the National Academy of Sciences - PNAS 115, 1162-1167, (2018). doi: 10.1073/pnas.1718453115

[11] CYGNSS. 2018. CYGNSS Level 2 Science Data Record Version 2.1. Ver. 2.1. PO.DAAC, CA, USA. Dataset accessed [2018-12-12] at https://doi.org/10.5067/CYGNS-L2X21.

[12] H. Hersbach, B. Bell, P. Berrisford, S. Hirahara, A. Horanyi, J. Muñoz-Sabater, J. Nicolas, et al., "Copernicus Climate Change Service (C3S) Climate Data Store (CDS)" , accessed 5 September 2023, doi: 10.24381/cds.adbb2d47